Size controlled synthesis of biocompatible gold nanoparticles and their activity in the oxidation of NADH

2012 Nanotechnology 23 015602

(http://iopscience.iop.org/0957-4484/23/1/015602)

Nanotechnology **23** (2012) 015602 (8pp) doi:10.1088/0957-4484/23/1/015602

Size controlled synthesis of biocompatible gold nanoparticles and their activity in the oxidation of NADH

Parvathy R Chandran[1], M Naseer[2], N Udupa[2] and N Sandhyarani[1]

[1] School of Nano Science and Technology, National Institute of Technology, Calicut, Kerala-673 601, India
[2] Manipal College of Pharmaceutical Sciences, Manipal University, Karnataka-576 104, India

E-mail: sandhya@nitc.ac.in

Received 19 September 2011, in final form 2 November 2011
Published 8 December 2011
Online at stacks.iop.org/Nano/23/015602

Abstract
Size and shape controlled synthesis remains a major bottleneck in the research on nanoparticles even after the development of different methods for their preparation. By tuning the size and shape of a nanoparticle, the intrinsic properties of the nanoparticle can be controlled leading tremendous potential applications in different fields of science and technology. We describe a facile route for the one pot synthesis of gold nanoparticles in water using monosodium glutamate as the reducing and stabilizing agent in the absence of seed particles. The particle diameter can be easily controlled by varying the pH of the reaction medium. Nanoparticles were characterized using scanning electron microscopy, UV–vis absorption spectroscopy, cyclic voltammetry, and dynamic light scattering. Zeta potential measurements were made to compare the stability of the different nanoparticles. The results suggest that lower pH favours a nucleation rate giving rise to smaller particles and higher pH favours a growth rate leading to the formation of larger particles. The synthesized nanoparticles are found to be stable and biocompatible. The nanoparticles synthesized at high pH exhibited a good electrocatalytic activity towards oxidation of nicotinamide adenine dinucleotide (NADH).

S Online supplementary data available from stacks.iop.org/Nano/23/015602/mmedia

(Some figures may appear in colour only in the online journal)

1. Introduction

As stable metal nanoparticles, gold nanoparticles have enormous applications in various fields of science and technology [1]. Gold nanoparticles are used in chemical [2] and biological sensors [3, 4], electronics [5], catalysis [6] and as carriers for drug delivery systems [7]. In the nanosize range the materials exhibit a transition between molecular and solid states, which make them interesting materials due to unique properties that in turn can be attributed to quantum confinement and surface effects [8]. There are two strategies for making metal nanoparticles: (a) a top-down approach and (b) a bottom-up approach, the latter being the most common and effective. In the bottom-up approach, the metal ions are reduced by a reducing agent that undergoes nucleation to form the nanoparticle in the presence of a protective ligand. Several modifications have been suggested in a wet chemical method for the synthesis of gold nanoparticles to give a more control of shape [9, 10] and size [11, 12]. Nowadays there is a tremendous increase in the application of gold nanoparticle in biomedical fields. A major factor that renders gold nanoparticles suitable for biomedical applications is their biocompatibility [13, 14]. Most of the properties exhibited by nanoparticles depend on their dimensions and morphology [15, 16]. Hence controlling the size of nanoparticles remains a challenging field.

Commonly used reducing agents for the synthesis of gold nanoparticles are tri-sodium citrate, ascorbic acid and sodium borohydride. Synthesis of gold nanoparticles using monosodium glutamate has also been reported [17]. In our study it was found that the size can be controlled by varying the pH of the precursor solution and reaction medium when

using glutamate as the reducing agent. However, such a change was not observed when other reducing agents such citrate are used. Detailed investigation on the characteristics of intermediates by UV–vis, zeta potential and dynamic light scattering (DLS) studies reveal the conversion of Au^{3+} to Au^{+}/Au^{2+} in the presence of glutamate; this further undergoes reduction/disproportionation to form Au^{0}. Higher reactivity of chloroauric acid at lower pH compared to higher pH favours the nucleation rate resulting in the formation of smaller particles. The different structures of glutamate at various pH values also support nucleation as well as stabilization of the nanoparticles. Through ligand exchange reactions these nanoparticles can be modified with polyethylene glycol (PEG) and other ligands with complete removal of the glutamate from the surface without affecting its size (see supplementary information available at stacks.iop.org/Nano/23/015602/mmedia). This makes the process more versatile and novel. These nanoparticles were studied for stability, biocompatibility and electrocatalytic activity. Interestingly an enhanced electrocatalytic activity was observed for the oxidation of glucose and nicotinamide adenine dinucleotide (NADH) using the nanoparticles prepared at pH 11.5 when compared with the nanoparticles prepared at other pHs.

2. Materials and methods

2.1. Chemicals

Chloroauric acid was purchased from SRL, India and monosodium glutamate was obtained from Loba Chemie, India. They were used as-received without any further purification. Deionized water was obtained using an ultrafiltration system (Milli-Q, Millipore) with a measured resistivity above 18 MΩ cm at 25 °C and passed through a 0.22 μm filter to remove particulate matter.

2.2. Synthesis of gold nanoparticles

Chloroauric acid and monosodium glutamate (MSG) were taken in a molar ratio of 1:7. To about 4 ml of 0.19 mM $HAuCl_4$, we added 100 ml distilled water and boiled the solution. When boiling commenced, 20 ml of 1.27 mM MSG was added. Formation of gold nanoparticles was manifested by the development of a red/pink colour. Heating was continued until the colour of the solution remains constant for about 1 min. Then the solution was rapidly cooled to room temperature. The initial pH of the solution was in the range of 2–3.

For controlled synthesis, the pH of the precursor chloroauric acid solution was changed using 0.1 M NaOH. After boiling, MSG is added and no considerable change in pH of the solution was observed. Whenever there was any change, the pH was adjusted using 0.1 M NaOH just after the addition of MSG and before the reduction commenced. The size and stability of the gold nanoparticles synthesized at different pH values were characterized by UV–vis spectrophotometry, cyclic voltammetry (CV), dynamic light scattering, zeta potential, transmission electron microscopy (TEM) and scanning electron microscopy(SEM).

3. Characterization

3.1. UV–vis spectrophotometry

The UV–vis spectrophotometric results reported here were all obtained using a Schimadzu 1800 UV–vis spectrophotometer. The measurements were made at room temperature with distilled water as the reference solution using a pair of quartz cuvettes with path length of 1 cm. Temperature dependence studies of the nanoparticles were done using a thermo-electrically temperature controlled cell holder, an attachment along with the UV–visible spectrophotometer, with a temperature control range of 7–60 °C. The temperatures of both sample and reference cells are controlled.

3.2. Scanning electron microscopy

The samples were prepared by drop-casting gold nanoparticle solutions on carbon tape which was then dried in a desiccator. A Hitachi SU6600 variable pressure field emission SEM operated at an accelerating voltage of 20 kV was used for taking the images.

3.3. Transmission electron microscopy

The samples were prepared by drop-casting dilute solutions of gold nanoparticles on carbon coated copper grids and drying. A Hitachi TEM operated at an accelerating voltage of 80 kV was used for taking the images.

3.4. Dynamic light scattering and zeta potential measurement

The size distribution and zeta potential of gold nanoparticles were evaluated by DLS measurement at 25 °C using a DLS system, Zetasizer nano series (Malvern, UK).

3.5. Cyclic voltammetry analysis

The CV studies were performed with CH 400A Electrochemical Quartz Crystal Microbalance (CH Instruments, Austin, TX, USA). A three electrode system comprising a platinum wire as the auxiliary electrode, Ag/AgCl as the reference electrode and platinum as the working electrode was used for the CV measurements. Different sized gold nanoparticles were drop casted on to the platinum working electrode and dried under a stream of nitrogen. Electrochemical measurements were carried out at room temperature with a scan rate 100 mV S^{-1} using 0.05 M H_2SO_4 as the electrolyte. For the electrocatalysis study a gold nanoparticle modified platinum electrode was used as the working electrode.

3.6. In vitro stability of gold nanoparticles

The critical coagulation concentration, the concentration of NaCl up to which the synthesized gold nanoparticles remain stable without any aggregation, was assessed by the addition of increasing concentrations of NaCl [18].

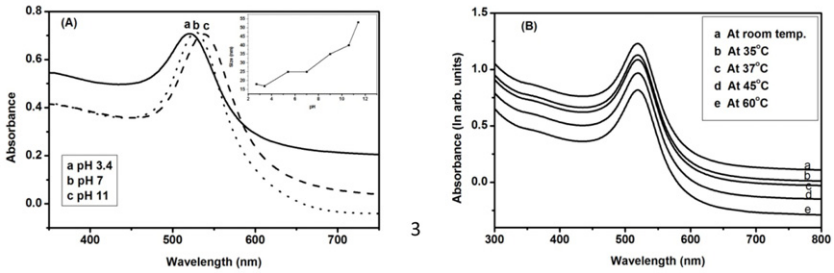

Figure 1. UV–vis spectra of (A) gold nanoparticles, namely (a) GNP1, (b) GNP2 and (c) GNP3. The inset shows the size of nanoparticles as a function of pH of the reaction medium. (B) GNP2 subjected to heating to 60 °C.

3.7. Cytotoxicity determination

The cytotoxic effects of the glutamate capped gold nanoparticles on RAW264.7 macrophage cells were studied by MTT assay [19]. Cells were cultured in Dulbecco's modified Eagle's medium (DMEM) with 10% foetal bovine serum (FBS) and 100 units ml^{-1} of penicillin and streptomycin in tissue culture flasks (T-25) in a humidified 37 °C CO_2 incubator (5% CO_2). Cells were monitored regularly in a phase contrast microscope. Healthy cells from the exponential growth phase were used for all the experiments.

The actively growing RAW264.7 cells were seeded at a density of 1×10^5 cells/well of a 96-well microtitre plate in triplicate and incubated in a humidified 37 °C CO_2 incubator (5% CO_2) for 24 h. 100 μl of freshly prepared concentrations (10, 20, 40 and 80 μM, by serial dilution) of glutamate reduced filtered gold nanoparticles in culture medium was added to the cells and further incubated for another 48 and 72 h under the conditions. Control cells were also used without the addition of gold nanoparticles. To evaluate cell survival or the toxicity level of gold nanoparticles, 20 μl of MTT solution (5 mg ml^{-1} in 1× phosphate buffered saline) was added to each well and incubated for 3 h. At the end of incubation period, medium containing MTT was gently replaced by 200 μl dimethyl sulfoxide to dissolve formazan crystals and the absorbance were measured by a microtitre plate reader (Biotek ELx800—MS) at 540 nm with a reference wavelength of 630 nm. The absorbance of test (treated cells) and the control (untreated cells) was used for the determination of the percentage cell viability. Cell survival in control cells was assumed to be 100%: % cell viability = OD of test/OD of control × 100 (OD is optical density). The IC50 (the concentration that gives 50% cell viability) value was determined from the graph.

4. Results and discussion

The nanoparticles were synthesized at various pH values from 3.4 to 11 and changes in size of the gold nanoparticles with pH of the reaction medium were observed. All other reaction parameters were kept the same. In most of the cases we obtained monodispersed particles. The inset of figure 1(A) shows the variation in size of the nanoparticles as a function of the pH of the medium. In this paper we report the features of the nanoparticles synthesized at three pH values, namely pH 3.4, 7 and 11, where distinct changes in size were observed. These are referred to as GNP1, GNP2 and GNP3, respectively. Figure 1(A) shows the UV–vis spectra of gold nanoparticles synthesized at three different pH values. It is clear from the spectra that by increasing the pH, the size of the glutamate stabilized gold nanoparticle also increased. The colloidal solutions of gold nanoparticles have an intense and characteristic ruby red colour due to the coherent oscillation of conductive electrons. These collective oscillations give rise to a specific surface plasmon absorption peak. Curve 'a' shows an absorption maximum at 520 nm and with the increase in pH there is a red shift in the peak which is also visible from the colour change of the solution from deep red to pink. Curves 'b' and 'c' have absorption maxima at 528 and 539 nm, respectively. The frequency and cross-section of the surface plasmon resonance (SPR) absorption and scattering are dependent on the metal composition, nanoparticle size and shape and dielectric properties of the surrounding medium or substrate [20]. With the variation in size of the nanoparticle, a shift in the SPR peak was observed.

The size and concentration of gold nanoparticles were also analysed theoretically using multipole scattering theory from the UV–vis spectra as reported by Haiss *et al* [21]. As per the proposed method, the ratio of the absorbance of the sample at the SPR peak to the absorbance at 450 nm will give the approximate size of the nanoparticles. The molar extinction coefficient at 450 nm as a function of size was given which was used for finding out the concentration of the samples. The concentration of nanoparticles decreases as the pH of the medium increase due to the increase in size of the particles (the concentration of precursor was taken as the same in all cases). The theoretical analysis also supported the experimental results. The data obtained from theoretical analysis were as shown in table 1.

To ascertain the stability of the synthesized nanoparticles at high temperatures, temperature dependent UV–vis absorption measurements were performed. These studies shows that the synthesized gold nanoparticles were stable up to 60 °C (figure 1(B)) without any aggregation. Being stable at a physiological temperature of 37 °C, the different sized glutamate stabilized gold nanoparticles can be used for biological applications.

SEM images confirm the particle sizes (table 1). In the SEM images the increase in the size of gold nanoparticles with increase in reaction pH is evident. This increase in

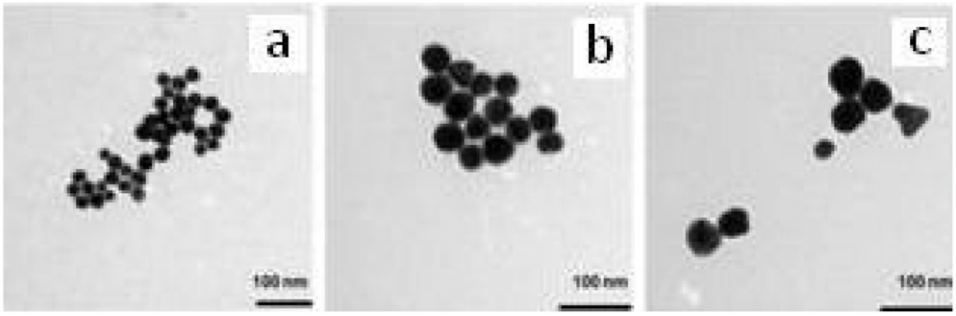

Figure 2. TEM images of (a) GNP1, (b) GNP2 and (c) GNP3.

Table 1. Size and concentrations of gold nanoparticles obtained from theoretical analysis of the SPR peak. The total gold ion concentration was the same in all cases.

Sample	pH of the solution	A_{spr}/A_{450}	ε_{450} (M^{-1} cm^{-1})	Size (nm)	Concentration (nM)
GNP1	3.4	1.677	5.93×10^8	17	0.593
GNP2	7	1.791	1.1×10^9	25	0.191
GNP3	11	2.05	1.19×10^{10}	53	0.02

size is responsible for the substantial increase in the longer wavelength absorption.

The size and morphology of the gold nanoparticles synthesized at various pH values were further verified by performing TEM measurements (figure 2). TEM study revealed that spherical particles were formed in most of the cases and the size of the particles increases as the pH of the reaction solution increases. At pH 3.4 the size of the particles was in the range 10–20 nm. At pH 7 and 11 the sizes were in the range 25–35 nm and 45–60 nm, respectively. Interestingly, nanoparticles synthesized at high pH show some nonspherical particles with facetted structures. These facetted structures are found to be a good electrocatalyst for NADH oxidation (see below).

4.1. Dynamic light scattering measurement

To further characterize the size of the gold nanoparticles and their stability at various pH values, DLS and zeta potential measurements were made. The results at various pH values reveal that the average hydrodynamic radius of the GNPs increases with increasing pH (table 2). The size profile obtained from the DLS system represents the hydrodynamic diameter of the particles. In accordance with the size measurements obtained from TEM imaging and theoretical methods, there was a corresponding increase of 10 nm for each sample in DLS measurement that can be attributed to the length of the ligands attached to the nanoparticle core along with the bound water molecules.

The surface charge of the nanoparticle systems was examined using ζ potential measurements, presented in table 2. We observed that the particles produced by this method were negatively charged for all the samples. The negative charge is attributed to the COO– charge of the glutamate on the surface of the nanoparticle. This is possible as the glutamate binds to the nanoparticle through the NH_2 group. There is faster reduction in the ζ potential value at lower pH, which leads to a decreased electrostatic repulsion between the particles and thereby lowers the stability of the particles. A minimum zeta potential of more than -60 is required for excellent stability, and of more than -30 for good physical stability [22]. Thus the zeta potential measurements show that the gold colloidal solution at pH 11 is more stable than the solutions at pH 7 and 3.4. In this case the reduction in the ζ potential value may be due to the lower pH which is comparable to the isoelectric point of the glutamate (which is 3.22). It is known that glutamate can exist in four different forms depending on the pH of the surrounding media [23]. These isoelectric forms were referred to by the global charge they carry such as $-2, -1, 0$ and $+1$. At a pH between 2.2 and 4.3 glutamate exists in its zwitterionic form, whereas at pH between 4.3 and 9.7 both carboxylic groups are deprotonated and the amine groups remain protonated and it carries a charge of -1. At a pH above 9.7 the global charge would be -2, with both carboxylic groups and amine groups deprotonated. The stabilization of gold nanoparticles by the different forms of glutamate at different pH determines the charge and zeta potential on the surface. Since the negative charge on the surface increases as pH increases, the zeta potential shows a higher negative value at higher pH.

4.2. Cyclic voltammetry analysis

It was reported that the metal nanoparticle oxidation should be size dependent because of a change in E^0 for the M^0/M^{n+} redox couple [24]. A negative shift in oxidation potential proportional to $1/r$ is predicted based on the change in Gibbs free energy associated with the increase in surface area [25]. Due to this difference in oxidation potential with size of the nanoparticle, CV or linear sweep voltammetry (LSV) could be used for the size analysis of the nanoparticle system. Here we

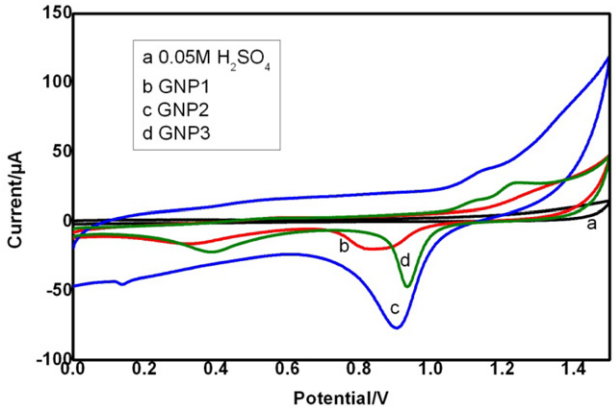

Figure 3. Cyclic voltammogram (CV) of a platinum electrode adsorbed with different sized gold nanoparticles in 0.05 M H_2SO_4 electrolyte.

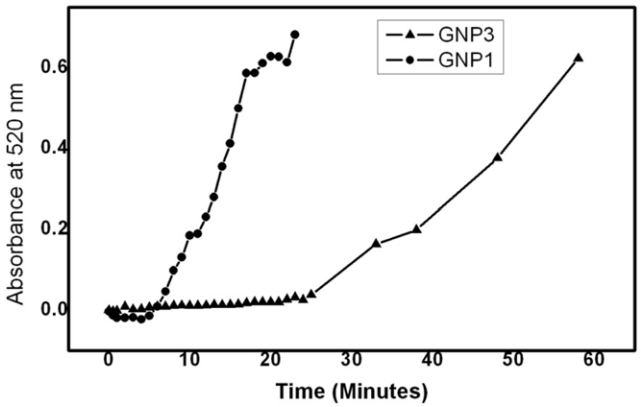

Figure 4. Kinetics of the formation of GNP1 and GNP3.

have used CV measurements as a confirmatory tool to support the size variation of the nanoparticles.

Figure 3 shows the cyclic voltammogram for the direct measurement of reduction potential for the oxidation of gold nanoparticles of different sizes. As supported by several theoretical [25] and experimental explanations [24], there was a negative shift in the reduction potential with the decrease in size. Multiple peaks were observed in GNP3 which are explained as due to the presence of facetted structures in the sample where different planes are exposed and oxidation takes place at different planes at different potentials.

A comparison of size obtained from various measurements is given in table 2.

4.3. Critical coagulation concentration (CCC)

Another important issue to be considered is the coagulation of gold nanoparticles at high salt concentration. Coagulation is promoted because of the compression of the electrical double layer by a high Na^+ ion concentration. The test was done by adding 200 mM of NaCl to a specified volume of gold nanoparticles. In this test NaCl solution was added until the plasmon absorption band remained the same as that of the initial solution, and it was found that the nanoparticles at pH 7 were stable up to a concentration of 34 mM of NaCl in 10 ml of solution. As this coagulation depends on the double layer charge we expected a variation in Na^+ concentration to induce coagulation to the three gold nanoparticles. Experiments confirmed the variation, where the gold nanoparticles at pH 3.4 showed a CCC of 26 mM of NaCl and at pH 11.7 a CCC of 36.7 mM. This again confirms the higher stability of the nanoparticles at pH 11.7, where the glutamate is in its doubly charged state.

4.4. Mechanism of nanoparticle growth

The mechanism for the reduction of chloroauric acid with glutamate will be a multistep process as suggested by the citrate reduction mechanism [26]. The proposed mechanism is as follows: reduction of chloroauric acid in the presence of glutamate leading to the formation of Au^0:

$$Au^{3+} + Glu \rightarrow Au^0 + Glu(ox)$$

$$Au^{3+} + Glu \rightarrow Au^{2+} + Glu(ox)$$

$$2Au^{2+} \rightarrow Au^+ + Au^{3+} \quad \text{(disproportionation reaction)}$$

$$3Au^+ \rightarrow 2Au^0 + Au^{3+} \quad \text{(disproportionation reaction)}$$

$$Au^+/Au^{2+} + Glu \rightarrow Au^0 + Glu(ox)$$

$$nAu^0 \rightarrow (Au^0)_n.$$

Formation of Au^+/Au^{2+} is confirmed from the colour and UV–vis spectrum (see supplementary information available at stacks.iop.org/Nano/23/015602/mmedia), during the first 5 min of the reaction. The yellow colour changes to colourless due to the formation of Au^+/Au^{2+}. The intensity of Au^{3+} decreases initially and then increases, supporting the suggested mechanism of disproportionation.

It was reported that the reactivity of chloroauric acid varies with the pH of the reaction medium [27]. At higher pH, chloroauric acid is present as a combination of gold chloro-hydroxy species and the reactivity of chloroauric acid decreases at higher pH due to the replacement of chloride ions by hydroxyl groups. This results in a decrease in the nucleation rate of the gold nanoparticles and an increase in growth rate, which leads to the formation of larger particles at higher pH. This was evident from the slow and gradual colour change, taking approximately 60 min for complete reduction to occur. The nucleation rate was higher in the case of lower pH as the chloride species is predominant at lower pH, and thereby there was a higher reactivity. Thus at lower pH the nucleation rate predominates over the growth rate and favours the formation of smaller particles.

The kinetic study was performed by analysing the absorbance spectra at different time intervals during the reaction. One millilitre of sample was withdrawn from the growth solution and the absorbance spectra was measured. The absorbance at 520 nm for the plasmon peak is plotted as a function of time for the high and low pH values (figure 4). It is observed that the reaction took only 20 min to complete the reduction at low pH.

Interestingly we observed that the nanoparticles synthesized at low pH values showed a broad plasmon peak which

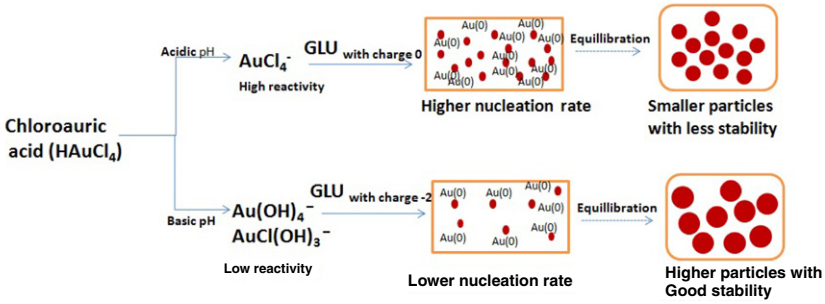

Scheme 1. Proposed mechanism for the nucleation and stabilization of nanoparticles at different pH values.

Table 2. Comparison of nanoparticle size obtained from SEM, UV and DLS. Peak potential from CV and zeta potential as a function of particle radius are tabulated.

Sample	pH of the solution	Size (nm) from DLS	Size (nm) from SEM	Size (nm) from UV	Experimental peak potential (V) from CV	Zeta potential
GNP1	3.4	35	10–20	17	0.85	−35
GNP2	7	45	25–35	25	0.90	−51
GNP3	11	75	45–60	53	0.92	−66.9

undergoes a blue shift and narrowing as the reaction proceeds. This suggests the formation of polydispersed samples at the beginning of the reaction which then equilibrate to form monodispersed particles (see supplementary information available at stacks.iop.org/Nano/23/015602/mmedia).

Scheme 1 shows the proposed mechanism for this observation.

The stabilization and growth rate can also be explained as due to the reactivity of the glutamate at different pHs. The isoelectric point of glutamate is 3.2, and it is noted in our experiment that the resulting nanoparticles aggregate when the pH of the mixture is lower than 3.2. It is known that below pH 2.2, the glutamate molecule will be fully protonated. The stabilization due to the positively charged amine group will be poor compared to the nonprotonated amine, which leads to the aggregation. As mentioned earlier in this paper, the different forms of glutamate at different pH conditions of the surrounding medium favour the growth rate and stabilization mechanism.

4.5. In vitro cytotoxicity

The cytotoxicity test was performed in order to evaluate the biocompatibility of gold nanoparticles and the potential for biological applications. Cell viability was evaluated by MTT assay using RAW264.7 macrophage cells. The result suggests that the cells retain viability up to 90% for both 48 and 72 h treatment at concentrations of 10 and 20 μM. However, at higher concentrations a decline in cell viability was observed (70–80% of cells are viable at a concentration tested of 80 μM). As shown in figure 5, all the concentrations tested for cytotoxicity were found to have considerably fewer toxic effects on the cells and the IC_{50} values could be above the maximum concentration tested (80 μM). However, a slight dose dependent decrease in cell viability was observed during the study.

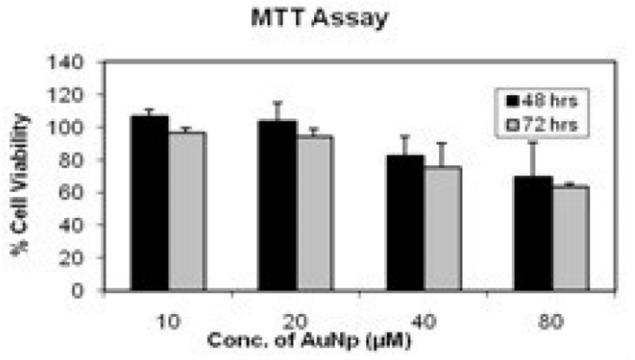

Figure 5. Cell viability induced by glutamate reduced gold nanoparticles after incubation for 48 and 72 h.

The results are contrary to certain reports showing the toxicity of Au(I) and Au(III) gold complexes [28, 29]. Our studies ensuring the biocompatibility of glutamate reduced gold nanoparticles are in strong agreement with the reports by other research groups. Studies done by Shukla *et al* [13] with borohydride reduced gold nanoparticles on similar macrophage cells (RAW 264.7) also suggest that Au(0) nanoparticles do not show any cytotoxic effects. Chithrani *et al* reported that the gold nanoparticles synthesized by a citrate reduction method are not cytotoxic and 98% of the cells remain viable even after the uptake of gold nanoparticles [14].

4.6. Electrocatalysis of GNP3 towards NADH oxidation

The electrochemical oxidation of NADH to enzymatically active NAD^+ has attracted considerable interest because over 300 dehydrogenases require NADH as a cofactor. It is reported that the formal potential of the $NADH/NAD^+$ couple in neutral pH at 25 °C is −0.56 versus SCE; however, a

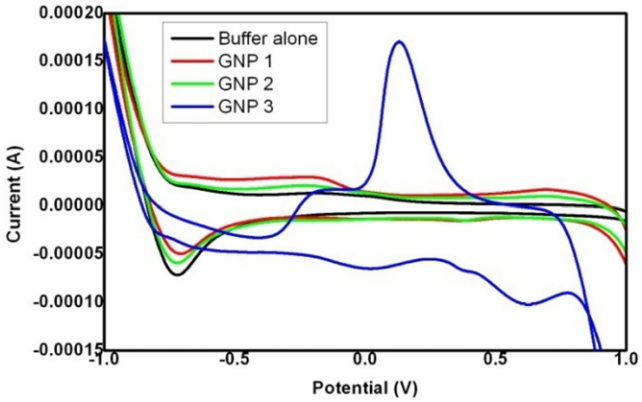

Figure 6. Cyclic voltammograms of NADH on a GNP modified platinum electrode in 0.1 M phosphate buffer solution.

significant overpotential as large as 1.0 V is often required for the oxidation at bare electrodes [30]. Due to this high potential, interference from other easily oxidizable species and fouling of electrode surface are major hurdles in the NADH detection. It is possible to reduce the overpotential by using a suitable electrocatalyst that can facilitate the electron transfer rate. For the potential application of the glutamate reduced nanoparticles in a biosensor, the electrocatalytic activity of all the three nanoparticles for NADH was investigated.

Figure 6 presents the cyclic voltammograms of NADH on gold nanoparticle modified platinum electrodes (the GNPs were drop casted on platinum electrode and allowed to dry under an IR lamp). The anodic peak potential of the GNP3 modified platinum electrode for NADH was at 0.12 V with a significant peak current, indicating that the GNP3 has good electrocatalytic activity for NADH oxidation. No characteristic response was observed with GNP1 and GNP2, which supports the earlier observations that the spherical structures do not catalyse the oxidation of NADH [31]. In the case of GNP3 none of the particles are spherical, demonstrating that the shape and surface structure play a predominant role in the electrocatalysis of NADH, which may be due to the exposed (111) planes.

The electrocatalytic activity of these particles towards glucose oxidation has also been studied, and it was found that the electrocatalytic activity is higher for GNP3 where a significant increase in peak current was observed in CV. Detailed investigations on the electrocatalytic nature of GNP3 and their application in biosensors are under way.

5. Conclusion

In this paper we have reported the facile and size controlled synthesis of gold nanoparticles by using glutamate as the reducing and stabilizing agent. The size of the resulting nanoparticles can be tuned by varying the pH of the reaction medium. The nanoparticles were stable and biocompatible. The nanoparticles synthesized at high pH exhibited a good electrocatalytic activity towards NADH oxidation and glucose oxidation, showing potential for application in biosensors. Complete ligand exchange with PEG thiol is possible without affecting the size, which shows great potential in biological applications like drug delivery.

Acknowledgment

PRC and NS thank Department of Biotechnology, Government of India for financial assistance.

References

[1] Daniel M C and Astruc D 2004 Gold nanoparticles: assembly, supramolecular chemistry, quantum-size-related properties, and applications toward biology, catalysis, and nanotechnology *Chem. Rev.* **104** 293–346
[2] Wang Z and Ma L 2009 Gold nanoparticles: assembly, supramolecular chemistry, quantum-size-related properties, and applications toward biology, catalysis, and nanotechnology *Coord. Chem. Rev.* **253** 1607–18
[3] Chah S, Hammond M R and Zare R N 2005 Gold nanoparticles as a colorimetric sensor for protein conformational changes *Chem. Biol.* **12** 323–8
[4] Elghanian R, Storhoff J J, Mucic R C, Letsinger R L and Mirkin C A 1997 Selective colorimetric detection of polynucleotides based on the distance-dependent optical properties of gold nanoparticles *Science* **277** 1078–81
[5] Shipway A N, Katz E and Willner I 2000 Nanoparticle arrays on surface for electronic, optical and sensor applications *ChemPhysChem* **1** 18–52
[6] Cortie M B and Lingen E V 2002 Catalytic gold nano-particles *Mater. Forum* **26** 1–14
[7] Han G, Ghosh P and Rotello V M 2007 Functionalized gold nanoparticles for drug delivery *Nanomedicine* **2** 113–23
[8] Alivisatos A P 1996 Perspectives on the physical chemistry of semiconductor nanocrystals *J. Phys. Chem.* **100** 13226
[9] He S, Zhang Y, Guo Z and Gu N 2008 Biological synthesis of gold nanowires using extract of rhodopseudomonas capsulata *Biotechnol. Prog.* **24** 476
[10] Chandran S P, Chaudhary M, Pasricha R, Ahmad A and Sastry M 2006 Synthesis of gold nanotriangles and silver nanoparticles using aloe vera plant extract *Biotechnol. Prog.* **22** 577–83
[11] Sau T K, Pal A, Jana N R, Wang Z L and Pal T 2001 Size controlled synthesis of gold nanoparticles using photochemically prepared seed particles *J. Nanopart. Res.* **3** 257–61
[12] Gao J, Bender C M and Murphy C J 2003 Dependence of the gold nanorod aspect ratio on the nature of the directing surfactant in aqueous solution *Langmuir* **19** 9065–70
[13] Shukla R, Bansal V, Chaudhary M, Basu A, Bhonde R R and Sastry M 2005 Biocompatibility of gold nanoparticles and their endocytotic fate inside the cellular compartment: a microscopic overview *Langmuir* **21** 10644–54
[14] Chithrani B D, Ghazani A A and Chan C W W 2006 Determining the size and shape dependence of gold nanoparticle *Nano Lett.* **6** 662–8
[15] Link S and El-Sayed M A 2003 Optical properties and ultrafast dynamics of metallic nanocrystals *Annu. Rev. Phys. Chem.* **54** 331–66
[16] Kelly K L, Coronado E, Zhao L L and Schatz G C 2003 The optical properties of metal nanoparticles: the influence of size, shape, and dielectric environment *J. Phys. Chem.* B **107** 668–77
[17] Dakua I, Sugunan A and Dutta J 2005 Gold nanoparticle synthesis from chloroauric acid reduction by monosodium glutamate *Proc. MRS Conf. (Boston)*
[18] Xie H, Tkachenko A G, Glomm W R, Ryan J A, Brennaman M K, Papanikolas J M, Franzen S and

Feldheim D L 2003 Critical flocculation concentrations, binding isotherms, and ligand exchange properties of peptide-modified gold nanoparticles studied by uv–visible, fluorescence, and time-correlated single photon counting spectroscopies *Anal. Chem.* **75** 5797–805

[19] Mosmann T J 1983 Rapid colorimetric assay for cellular growth and survival: application to proliferation cytotoxicity assays *Immunol. Methods* **65** 55–63

[20] Mie G 1908 Considerations on the optic of turbid media, especially colloidal metal sols *Ann. Phys.* **25** 377–442

[21] Haiss W, Thanh N T, Aveyard J and Fernig D G 2007 Determination of size and concentration of gold nanoparticles from UV–vis spectra *Anal. Chem.* **79** 4215–21

[22] Riddick T M 1968 Control of colloidal stability through zeta potential *Zeta-Meter Manual* (New York: Zeta-Meter Manual)

[23] Edshall J T and Wyman J 1958 *Biophysical Chemistry* (New York: Academic)

[24] Ivanova O S and Zamborini F P 2010 Electrochemical size discrimination of gold nanoparticles attached to glass/indium-tin-oxide electrodes by oxidation in bromide-containing electrolyte *Anal. Chem.* **82** 5844–50

[25] Plieth W J J 1982 Electrochemical properties of small clusters of metal atoms and their role in the surface enhanced Raman scattering *Phys. Chem.* **86** 3166–70

[26] Kumar S, Gandhi K S and Kumar R 2007 Modelling of formation of gold nanoparticles by citrate method *Indust. Eng. Chem. Res.* **46** 3128–36

[27] Goia D V and Matijevic E 1999 Tailoring the particle size of monodispersed colloidal gold *Colloid Surf.* A **146** 139–52

[28] Griem P and Gleichmann E Z 1996 Gold antirheumatic drug: desired and adverse effects of Au(I) and Au(III) on the immune system *Rheumatol.* **55** 348–58

[29] Mirabelli C K, Johnson R K, Sung C M, Faucette L, Muirhead K and Crooke S T 1985 Evaluation of the *in vivo* antitumor activity and *in vitro* cytotoxic properties of auranofin, a coordinated gold compound, in murine tumor models *Cancer Res.* **45** 32–39

[30] Gorton L, Dominguez E and Wilson G S (ed) 2002 *Electrochemistry of* $NAD(P)^+/NAD(P)H$*, Encyclopedia of Electrochemistry* (*Bioelectrochemistry* vol 9) (Weinheim: Wiley-VCH)

[31] Das A K and Raj C R 2011 Rapid room temperature synthesis of electrocatalytically active Au nanostructures *J. Colloid Interface Sci.* **353** 506–11